



Comparative Study of Radioactivity and Afterheat in Several Fusion Reactor Blanket Designs

R.W. Conn, T.Y. Sung, and M.A. Abdou

October 1974

UWFDM-113

***FUSION TECHNOLOGY INSTITUTE
UNIVERSITY OF WISCONSIN
MADISON WISCONSIN***

**Comparative Study of Radioactivity and
Afterheat in Several Fusion Reactor Blanket
Designs**

R.W. Conn, T.Y. Sung, and M.A. Abdou

Fusion Technology Institute
University of Wisconsin
1500 Engineering Drive
Madison, WI 53706

<http://fti.neep.wisc.edu>

October 1974

UWFDM-113

Comparative Study of Radioactivity and
Afterheat in Several Fusion Reactor
Blanket Designs

by

R. W. Conn

T. Y. Sung

Nuclear Engineering Department
University of Wisconsin
Madison, Wisconsin 53706

and

M. A. Abdou

Argonne National Laboratory
Argonne, Illinois

October, 1974

FDM-113

Abstract

The induced radioactivity and afterheat in five recently presented fusion reactor blanket designs have been calculated. These designs differ in the choices of structural material. Nevertheless, the radioactivity levels and in the use of a neutron multiplier and yet the radioactivity levels at shutdown after two years of operation are within a factor of four of each other and clustered about $1 \text{ Ci/W}_{\text{th}}$. However, the long term radioactivity (greater than 200 years) is greatest for Nb structures and least for Al. For Nb, the level of long term activity is about $5 \times 10^{-5} \text{ Ci/W}_{\text{th}}$ whereas for Al, the level drops to approximately $10^{-7} \text{ Ci/W}_{\text{th}}$ just several weeks after shutdown. This last result will be modified by the inclusion of trace elements and impurities. Afterheat levels are found to vary from 1/2 to 5 percent of the thermal operating power, depending on design and the choice of structural material. Importantly, however, the afterheat power density is only about 0.2 W/cm^3 at most and this is roughly a factor of 10 to 60 less than the afterheat power density in fast breeder reactors. BHP values are calculated for all designs by the pessimistic approach of dividing the activity in Ci/kW_{th} by the lowest MPC value, in Ci/km^3 of air presented in A.E.C. rules, title 10, part 20. In all cases, the BHP nevertheless drops below $1 \text{ km}^3/\text{kW}_{\text{th}}$ 20 years after shutdown following two years of operation. The key isotopes contributing to radioactivity, afterheat, and BHP are listed for future reference.

I. Introduction

Radioactivity and afterheat resulting from neutron induced reactions will be an important consideration in the design of future controlled thermonuclear fusion systems, particularly those based on the deuterium-tritium fusion reaction. There have recently been several analyses of this problem for particular fusion reactor blanket designs.⁽¹⁻⁵⁾ In addition, there have been studies of radioactivity and afterheat reported as part of several rather complete conceptual designs of fusion power reactors.⁽⁶⁻¹¹⁾ It appears from the results of these initial studies that D-T fueled fusion systems will have induced radioactivity levels on the order of 10^6 Ci/MW_{th}, that afterheat levels at shutdown will be about 1% of operating power, and that particular structural materials, namely aluminum⁽¹⁰⁾ and vanadium⁽¹²⁾ based alloys, appear particularly promising from the viewpoint of minimum long term radioactivity.

With the appearance recently of relatively complete conceptual fusion reactor designs,⁽⁶⁻¹⁰⁾ (in some sense, a first generation set of designs), it is of interest to examine comparatively the radioactivity and afterheat in these systems. It is of particular interest to study the impact of different choices for the structural material and to see if the different blanket designs themselves have any real affect on the radioactivity and afterheat levels. A previous paper by two of the authors⁽¹³⁾ has already investigated other important characteristics of these systems, such as tritium breeding ratio, nuclear heating, and gas production and atom displacement rates. Thus, these papers together constitute a fairly complete comparative study of the neutronics related aspects of these five fusion blanket designs.

II. Blanket Designs and Calculational Procedure

The blanket designs studied here were developed as part of an overall conceptual design of a fusion reactor by groups at the University of Wisconsin,⁽⁶⁾ the Oak Ridge National Laboratory (ORNL)⁽⁷⁾, the Princeton Plasma Physics Laboratory (PPPL)⁽⁸⁾, the Lawrence Livermore Laboratory (LLL)⁽⁹⁾, and the Brookhaven National Laboratory (BNL)⁽¹⁰⁾. Table I summarizes these designs in a format used for the neutronics calculations. The Wisconsin design,⁽⁶⁾ called UWMAK-I, and the LLL design⁽⁹⁾ both use 316 type stainless steel as the structure and liquid lithium as the coolant, moderator, and tritium breeding material. Natural lithium is used in UWMAK-I while the lithium in the LLL blanket is depleted to 4 a/o ^6Li . The PE-16 alloy used as the structure in the PPPL blanket⁽⁸⁾ is approximately 43 w/o nickel, 39 w/o iron, and 18 w/o chromium. The coolant is helium and the moderating and breeding material is flibe (LiF-BeF_2). The ORNL blanket⁽⁷⁾ uses niobium, a refractory metal, as the structural material, natural lithium for cooling and breeding, and is designed for very high temperature operation. The BNL design is based on SAP, (sintered aluminum product) a material in which pure aluminum is strengthened by the addition of 5 to 10 w/o Al_2O_3 finely dispersed throughout the aluminum matrix. SAP was originally proposed for fusion reactors by Powell et.al.⁽¹⁰⁾ on the basis of its low long term radioactivity. The breeding material is LiAl , a solid material, and the coolant is helium. Be is included for neutron multiplication and the lithium is enriched to 90a/o ^6Li to increase tritium production.

Neutron transport calculations for each of these systems were performed using the ANISN program⁽¹⁴⁾ in the $S_8\text{-P}_3$ approximation as described earlier.⁽¹³⁾ In all cases, the nuclear data for the transport calculations are from ENDF/B3 and have been processed using

the programs SUPERTOG⁽¹⁵⁾ and MUG⁽¹⁶⁾. Other cross sections relevant to radioactivity and afterheat calculations were also obtained from ENDF/B3 and processed with the MACK program.⁽¹⁷⁾ The exceptions are the neutron cross sections for fluorine which are from the GAM-II library⁽¹⁸⁾ and some calculated cross sections for radioactive nuclides provided by BNL.⁽¹⁹⁾ In addition, cylindrical geometry is used for the UWMAK-I, ORNL, PPPL, and BNL designs. The LLL design is for application to a mirror confinement system and spherical geometry is used. The resulting neutron fluxes were used to calculate the induced radioactivity in each system. Double capture events are generally not included because of the low fluxes in these systems. Exceptions to this, however, include the double capture on ^{58}Ni , which is important in stainless steel systems, and several successive captures in niobium. Further, several reactions can lead to metastable states in the product nucleus. Important examples are the (n,γ) reaction in ^{93}Nb leading to $^{94\text{m}}\text{Nb}$ (spin 3, $t_{1/2} = 6.26 \text{ m}$) and ^{94}Nb (spin 6, $t_{1/2} = 2 \times 10^4 \text{ y}$) and the $(n,2n)$ reaction on ^{27}Al leading to ^{26}Al (spin 5, $t_{1/2} = 7.4 \times 10^5 \text{ y}$) and $^{26\text{m}}\text{Al}$ (spin 0, $t_{1/2} = 6.4 \text{ s}$). For this last reaction, the branching ratio is taken as 0.5.

In general, the branching ratio to such product nuclei is not well known and various authors have made different assumptions.^(1,4,5) We have therefore considered two different cases for Nb and the sensitivity of the results to such assumptions will be discussed shortly. An additional difficulty is that the capture cross section of ^{94}Nb is not well known. This reaction transmutes the long lived isotope ^{94}Nb to ^{95}Nb and $^{95\text{m}}\text{Nb}$, both of which have short half lives. Since the thermal capture cross section and the resonance integral^(20,21) of ^{94}Nb are about 15 times the corresponding values for ^{93}Nb , several previous studies^(1,5) have assumed $\sigma(n,\gamma)$ for

^{94}Nb to be 15 times $\sigma(n,\gamma)$ in ^{93}Nb . This, however, clearly remains conjecture. Depending on exposure time, this assumption may predict too much burnout of ^{94}Nb and lead to high ^{95}Nb and $^{95\text{m}}\text{Nb}$ concentrations.

Muir and Dudziak⁽²²⁾ have recently examined the sensitivity of afterheat and radioactivity in the Reference Theta Pinch Reactor (RTPR)⁽¹¹⁾ to the uncertainty in the $^{94}\text{Nb}(n,\gamma)$ cross section. They have constructed hypothetical cross sections which tend to minimize or maximize the capture rate while preserving the value of the resonance integral at 125 barns above 50 eV. They have found that the "times fifteen" assumption overpredicts afterheat (by burning ^{94}Nb to $^{95\text{m}}\text{Nb}$) and therefore yields lower values for the long term radioactivity. They give results only at shutdown and find differences can be as much as 60% for 5 year and longer exposures. We have considered only the sensitivity to the "times fifteen" assumption on $^{94}\text{Nb}(n,\gamma)$ after 2 year exposure and find that the only significant change occurs at times close to the half life of ^{95}Nb , namely around 35 days after shutdown. Both the short term (less than 1 week) and the long term (greater than 1 year) radioactivity is found to be insensitive (within 3%) to these two possibilities.

III. Results and Discussion

A comparison of radioactivity in the five systems outlined in Table I is given in Figure 1 following shutdown after two years of operation. The two year operating time has been consciously chosen in light of recent studies^(1,23) of the radiation damage to fusion reactor structural materials which have shown that in the designs studied here, the expected life of the first wall (and the first 20 cm of the blanket thickness) will be approximately two years for a 14 MeV neutron wall loading of 1 MW/m^2 ,

This means the blanket segments must be removed and this first 20 cm replaced in order to insure integrity of the blanket structure. There has been a recent proposal for blanket designs which can extend the life of the structural material⁽²⁴⁾ but these concepts were not employed in the blanket design studies here. As such, operating times longer than two years would not be consistent with the radiation damage analysis. The effect, however, may be of interest and we refer to reference 4 for a discussion of radioactivity and afterheat in a specific fusion reactor design where results were computed following 10 years of operation.

The radioactivities shown in Figure 1 have been divided by the thermal operating power to provide a basis for comparison. At shutdown, the radioactivity levels are within a factor of four of each other and clustered about a value of 10^6 Ci/MW_t. However, after only several weeks, the radioactivity in the aluminum based BNL design has dropped by more than six orders of magnitude. The radioactivity in the two stainless steel systems and the high nickel based alloy, PE-16, system of PPPL are about the same. The somewhat higher radioactivity in the PPPL design is due in large part to the thicker first wall in that system. The niobium ORNL system has the highest radioactivity levels at times greater than 200 years because of the ^{94}Nb ($T_{1/2} = 2 \times 10^4$ y) activity.

The radioactivity in the first wall is a dominant contributor to the overall radioactivity. As such, we have tabulated in Tables 2A through 2E the major isotopes leading to the radioactivity in this zone. One can thus

readily see which isotopes are the major contributors at various times after shutdown. In the UWMAK-I, PPPL and LLL designs, the short term activity is dominated by ^{55}Fe ($T_{1/2} = 2.6 \text{ y}$) while at long times, the main isotopes are ^{63}Ni ($T_{1/2} = 92 \text{ y}$), ^{53}Mn ($T_{1/2} = 2 \times 10^6 \text{ y}$) and ^{59}Ni ($t_{1/2} = 8.4 \times 10^4 \text{ y}$). In the niobium system of ORNL, the short term activity is dominated by $^{92\text{m}}\text{Nb}$ ($t_{1/2} = 10.14 \text{ d}$) while the long term activity comes from ^{94}Nb ($t_{1/2} = 2 \times 10^4 \text{ y}$). For the BNL system, ^{24}Na ($t_{1/2} = 15 \text{ h}$) and ^{27}Mg ($t_{1/2} = 9.5 \text{ m}$) dominate at early times while ^{26}Al ($t_{1/2} = 7 \times 10^5 \text{ y}$) is the main long term contributor. Note that some of these decays are by nuclear capture of atomic electrons and, as with ^{55}Fe , may not emit any gammas. Such decays, while contributing to the curie level, do not pose a biological hazard. This will be brought out shortly in a comparison of biological hazards potential.

Turning now to a discussion of afterheat, a comparison is shown in Figure 2 with the afterheat given as a percentage of the thermal operating power. The values at shutdown differ by more than a factor of 10. The UWMAK-I and LLL stainless steel designs yield approximately the same results while the PPPL results are higher. This is again due to the thicker first wall in that design and to the higher Ni content. The low value of afterheat in the niobium ORNL system is partly due to the low percentage of structural material (1%) in the tritium breeding zone compared to the other designs. (See zone 4 of the ORNL design in Table I.) This, of course, also affects the radioactivity results for that system.

Since the short times immediately following shutdown are most relevant for accident studies, we present in Figure 3 a plot of afterheat at times from 0.6 sec to 100 min shutdown. The niobium system, which has the best high temperature properties, has the lowest afterheat values at early times. Conversely, the aluminum based SAP system has a relatively high afterheat value, about 2% of the thermal operating power, and it remains roughly constant at this value for several minutes after shutdown. Since SAP does not have the good high temperature properties of either stainless steel or refractory metals, this is an important point to note.

The afterheat plotted in Figure 3 is the total afterheat in the blanket and shield. We have not presented detailed space dependent heating rates. As such, gammas produced on radioactive decay are assumed to deposit their energy at the point of origin. For a specific study of a particular accident situation, one would of course transport the gammas to determine the exact space dependent heating. It should be noted, however, that the maximum power density in a fusion reactor blanket during operation is typically between 10 and 20w/cm³. This is roughly ten times lower than the power density in light water fission reactors and a factor of 60 less than the power density in a fast breeder reactor. Therefore, the afterheat power density in fusion reactor blankets will be 10 to 60 times less than that in fission reactors even though the total afterheat at shutdown is similar for both systems.

Another relevant comparison between these systems is shown in Figure 4 where the biological hazard potential (BHP) is given as a function of time after shutdown. The BHP is defined as the activity in curies per thermal watt divided by the maximum permissible concentration (MPC) in Ci per km³ of air.

For consistency, we have used in all cases the lowest MPC values from U.S.A.E.C. rules, title 10, part 20. The high values for the niobium system at early times come from ^{92m}Nb for which the rules as stated in title 10, part 20 have been applied. The rules require the MPC value to be 10^{-10} $\mu\text{Ci/ml}$ since this nuclide is not explicitly listed. However, ^{92m}Nb decays primarily by electron capture and has a relatively short half life. A similar isotope, ^{58}Co , which also decays primarily by electron capture and has a longer half life than ^{92m}Nb , is assigned an MPC value of 3×10^{-8} $\mu\text{Ci/ml}$. For these reasons, the MPC value for ^{93m}Nb should actually be between 10^{-7} to 10^{-8} $\mu\text{Ci/ml}$. Previous authors^(1,5) have in fact used estimated MPC values in this range and the corresponding BHP values are much reduced. We have shown this in Figure 4 by including a BHP curve for the ORNL system using an MPC value of 3×10^{-7} $\mu\text{Ci/ml}$ for ^{92m}Nb . The authors believe this latter case reflects the actual situation more realistically and that this will be supported when A.E.C. rules and regulations, title 10, part 20, are made to explicitly include an evaluated MPC value for ^{92m}Nb . Returning to the discussion of Figure 4, note that the aluminum and stainless steel systems are fairly close in value at shutdown but after one week, as with the comparison of radioactivity, the SAP system of BNL has much smaller values than any other system.

To examine the sensitivity of these results to the assumed branching ratio, we have examined two cases for Nb. In the first case, we assumed the (n,2n) reaction in $^{93}_{41}\text{Nb}$ branches two thirds of the time to ^{92m}Nb and one third of the time to ^{92}Nb . Captures in ^{93}Nb and ^{94}Nb are assumed to lead to the metastable state 90% of the time. These branching schemes have been used by other authors previously.^(1,4,5) For a comparative case, we have assumed all branching ratios are 0.5. The results for radioactivity and afterheat are given in Table 3. Clearly, the first case gives conservative results since it produces

the metastable state more frequently, thus adding to the short time activity. Yet it will yield the same long term activity as the second case since the metastable state simply decays to the longer lived ground state. Interestingly, while the radioactivity can be higher by ~40%, the afterheat using either branching ratio assumption is much less sensitive. The reason is the low average decay energy associated with ^{94m}Nb and ^{95m}Nb .

In summary, all these designs have radioactivity levels of about 10^6 Ci/MW_t at shutdown after two years of operation. The aluminum based structure⁽¹⁰⁾ is clearly best from the viewpoint of long term radioactivity with values of about 0.1 Ci/MW_t at times greater than a few weeks following shutdown. The niobium structure, on the other hand, may have radioactivity levels on the order of 100 Ci/MW_t even after 2000 years. However, definitive results here must await better measurement of the capture cross section of ^{94}Nb and the determination of the proper branching ratio for the $^{93}\text{Nb}(n,\gamma)$ reaction. Afterheat levels in these systems differ by more than a factor of 10 at shutdown with the PE-16 design of PPPL and the SAP design of BNL being the highest. The thicker first wall in the PPPL design to some extent accounts for the higher value in that system as compared to stainless steel systems. The high afterheat in the SAP system is approximately 2% of the thermal operating power which can be important in accident situations since SAP does not have good high temperature properties. The niobium design of ORNL has the lowest afterheat at shutdown but this is partly due to the design choice of low percentage structure (1%) in the tritium breeding zone. Other designs typically used a value of 5% or more for the percentage of structural material. Compared

on the basis of BHP, the niobium system has the highest value at long times after shutdown (because of ^{94}Nb) while the BHP values of a SAP system become extremely small in just several weeks. The values for the SAP system may increase sharply, however, when trace elements and impurities are included.

Acknowledgement

This research was supported by grants from the U.S.A.E.C. and the Wisconsin Electric Utility Research Foundation.

References

1. D. Steiner, "The Neutron Induced Activity and Decay Power of the Niobium Structure of a D-T Fusion Reactor Blanket," (ORNL-TM-3094, Oak Ridge National Laboratory, 1970).
2. S. Blow, J. Brit. Nucl. Eng. Soc. 11, 371 (1972).
3. D. Steiner and A.P. Fraas, Nucl. Safety. 13, 353 (1972).
4. W. F. Vogelsang, G. L. Kulcinski, R. G. Lott and T. Y. Sung, Nucl. Tech., 22, 379 (1974).
5. D. J. Dudziak and R. A. Krakowski, "A Comparative Analysis of D-T Fusion Reactor Radioactivity and Afterheat," in Proc. First Top. Meet. on Tech. of Cont. Nucl. Fus. (CONF-740402-P1, U.S.A.E.C.) 1, 548 (1974).
6. B. Badger, et al., "A Wisconsin Tokamak Reactor Design, UWMAK-I," (UWFDM-68, Nuclear Eng. Dept., University of Wisconsin, Nov. 1973.)
7. A. P. Fraas, "Conceptual Design of the Blanket and Shield Region and Related Systems for a Full Scale Toroidal Fusion Reactor," (ORNL-TM-3096, Oak Ridge National Lab., May 1973.)
8. W. G. Price, Jr., Trans, Am. Nucl. Soc. 17, 35 (1973). Also, W. G. Price, private communication.
9. J. D. Lee, "Geometry and Heterogeneous Effects on the Neutronics Performances of a Yin-Yang Mirror Reactor Blanket," (UCRL-75141, Lawrence Livermore Laboratory, 1973). Also, J. D. Lee, private communication.
10. J. R. Powell, F. T. Miles, A. Aronson, and W. E. Winsche, "Studies of Fusion Reactor Blankets with Minimum Radioactive Inventory and with Tritium Breeding in Solid Lithium Compounds," BNL-18236, Brookhaven National Laboratory (June, 1973). (Design #4A, p. 79).
11. "An Engineering Design Study of a Reference Theta-Pinch Reactor (RTPR)," LA-5336; ANL-8019. Joint Report of Los Alamos Sci. Lab. and Argonne National Lab. (March, 1974).
12. D. Steiner, Nucl. Fus. 14, 33 (1974).
13. M. A. Abdou and R. W. Conn, Nucl. Sci. Eng. 55, 256 (1974).
14. W. W. Engle, Jr., "A User's Manual for ANISN," K-1693, Oak Ridge Gaseous Diffusion Plant (March 1967).
15. R. Q. Wright et al., "SUPERTOG: A Program to Generate Fine Group Constants and Pn Scattering Matrices from ENDF/B," ORNL-TM-2679 (1969)

16. J. R. Knight and F. R. Mynatt, "MUG: A Program for Generating Multigroup Photon Cross Sections," CTC-17, (Jan. 1970).
17. M. A. Abdou and C. W. Maynard, Trans. Am. Nucl. Soc. 16,129 (1973).
18. GAM-II Cross Section Library. Data Available from R.S.I.C., Oak Ridge National Laboratory.
19. S. Pearlstein, private communication. See also, S. Pearlstein, J. Nucl. En. 27, 81 (1973).
20. G. E. Moore (ed.). "Chemistry Division Annual Progress Report," ORNL-4306, Oak Ridge National Laboratory (1968).
21. R. M. Brugger and R. L. Heath (eds.), "Nuclear Technology Branch Annual Report," IN-1317, Idaho Nuclear Corp. (1970).
22. D. W. Muir and D. J. Dudziak, Trans. Am. Nucl. Soc. (in press).
23. G. L. Kulcinski, R. G. Brown, R. G. Lott, and P. A. Sanger, Nucl. Tech. 22, 20 (1974).
24. R. W. Conn et al., "New Concepts for Controlled Fusion Reactor Blanket Design," Nuclear Technology (in press, June 1975).

Figure Captions

Fig. 1 - Radioactivity as a function of time after shutdown following two years of operation for the five designs studied.

Fig. 2 - Afterheat as a function of time after shutdown following two years of operation in the five designs studied.

Fig. 3 - Afterheat at short times after shutdown. The low values for Nb are partly due to the low percentage structure assumed in the ORNL design.

Fig. 4 - BHP values as a function of time after shutdown following two years of operation. The MPC values are in $\mu\text{Ci/ml}$. The reason for the two values for $^{92\text{m}}\text{Nb}$ are discussed in the text.

Table 1
Description of Various Blanket Designs*

zone	UWMAK-I ⁽⁶⁾ (Cylindrical Geometry)		ORNL ⁽⁷⁾ (Cylindrical Geometry)	
	outer radius (cm)	Composition†	outer radius (cm)	Composition†
1	500	Plasma	280	Plasma
2	550	Vacuum	350	Vacuum
3	550.4	Stainless Steel ^b	350.25	Niobium
4	567.4	95% Li + 5% SS	380.25	99% Li + 1% Nb
5	584.4	95% Li + 5% SS	380.5	Niobium
6	601.4	95% Li + 5% SS	420.5	Graphite
7	616.4	Stainless Steel	420.75	Niobium
8	621.4	95% Li + 5% SS	450.75	99% Li + 1% Nb
9	623.4	Stainless Steel	451.0	Niobium
	PPPL ⁽⁸⁾ (Cylindrical Geometry)		LLL ⁽⁹⁾ (Spherical Geometry) ^a	
	outer radius (cm)	Composition†	outer radius (cm)	Composition†
1	290	Plasma	320	Plasma
2	360	Vacuum	480	Vacuum
3	366	16.4% PE-16	480.1	Stainless Steel ^b
4	376	0.731% Flibe + 5.7% PE-16	481	Lithium
5	376.36	PE-16	490	85% Li + 5% SS
6	388.36	78.8% Flibe + 4.5% PE-16	510	85% Li + 5% SS
7	388.72	PE-16	510.9	Lithium
8	408.72	82.0% Flibe + 3.8% PE-16	511	Stainless Steel
9	409.09	PE-16	512	Graphite
10	439.64	91.2% Flibe + 3.8% PE-16	540	40% Li + 40% C + 10% SS
11	440.0	PE-16	580	40% Li + 40% C + 10% SS

(continued on next page)

Table 1

Continued

BNL ⁽¹⁰⁾ (Cylindrical Geometry) ^a		
1	250	Plasma
2	300	Vacuum
3	302	SAP (sintered aluminum product)
4	332	17% SAP + 11% Al ₂ O ₃ + 10% Li Al + 45% Be + 17% He
5	357	20% SAP + 11% Al ₂ O ₃ + 10% Li Al + 42% C + 17% He
6	382	20% SAP + 11% Al ₂ O ₃ + 10% Li Al + 42% C + 17% He
7	462	(Shield) 20% SAP + 11% Al ₂ O ₃ + 52% Ti H _{1.5} + 17% He

a - The UWMAK-I, ORNL, and PPPL designs utilize natural lithium (7.56% ⁶Li). In LLL design the lithium is depleted to 4.0% ⁶Li and in BNL design lithium is enriched to 90% ⁶Li.

* All these blankets were followed by shields. While these shields were included in our calculations, their description is not given here as they do not significantly affect the results.

† All composition percentages are by volume.

b In the UWMAK-I design the composition of stainless steel was taken as 0.06, .014, and 0.009x10²⁴ atoms/cm³ for Fe, Cr, and Ni respectively. In the LLL design the atomic densities per cm³ were taken as .0672x10²⁴ for iron and 0.0168x10²⁴ for chromium plus nickel.

TABLE 2A
 SPECIFIC RADIOACTIVITY IN FIRST WALL (ZONE 3) OF UWMK-I
 (In disintegrations per sec per cm³ for 1 MW/m² wall loading; After 2 year operation)

		TIME AFTER SHUTDOWN							
Nuclide	Half-life	0	10 M	1.7 Hrs	2 yrs	20 yrs	200 yrs	2000 yrs	
⁵⁵ Fe	2.6 y	.946 + 12*	.946 + 12	.946 + 12	.570+12	.594+10			
⁵¹ Cr	27.8 d	.421 + 12	.421 + 12	.420 + 12					
⁵⁴ Mn	303 d	.223 + 12	.223 + 12	.223 + 12	.449+11				
⁵⁷ Co	270 d	.897 + 11	.897 + 11	.897 + 11	.151+11				
⁶⁰ Co	5.26Y	(.222 + 11)	(.222 + 11)	(.222 + 11)	.173+11	.180+10			
^{60m} Co	10.5 m	.571 + 11	.290 + 11						
⁵⁸ Co	71.3 d	.316 + 12	.316 + 12	.316 + 12					
⁵⁶ Mn	2.58h	.628 + 12	.601 + 12	.401 + 12					
⁵² V	3.7 m	.136 + 12							
²⁸ Al	2.3 m	.427 + 11							
⁶³ Ni	92 y								
⁵⁹ Ni	8x10 ⁴ y					.134+9	.369+8	.169+6 .253+5	
⁵³ Mn	2x10 ⁶ y								
TOTAL	[DPS/cm ³]	.294 + 13	.270 + 13	.244 + 13	.649+12	.787+10	.371+8	.194+6	

*Numbers in all tables, 2A-2E, should be read as $a \pm n = a \times 10^{\pm n}$

TABLE 2B

Specific Radioactivity in First Wall (Zone 3) of ORNL Design
(In disintegrations per sec per cm^3 for 1 MW/m^2 wall loading; After 2 year operation)

		TIME AFTER SHUTDOWN						
Nuclide	Half-Life	0	10M	1.7 hrs.	2 yrs	20 yrs	200 yrs	2000 yrs
$^{92\text{m}}\text{Nb}$	10.14 d	.681+13	.681+13	.678+13				
$^{94\text{m}}\text{Nb}$	6.26 m	.223+13	.734+12					
^{90}Y	64 h	.932+11	.930+11	.915+11				
$^{95\text{m}}\text{Nb}$	90 h			.729+11				
$^{93\text{m}}\text{Nb}$	13.6 y				.903+10	.378+10		
^{94}Nb	2×10^4 y				.175+9	.175+9	.174+9	.164+9
TOTAL [DPS/cm ³]		.928+13	.778+13	.702+13	.920+10	.396+10	.175+9	.164+9

TABLE 2C

Specific Radioactivity in First Wall (Zone 3) of PPPL Design

(In disintegrations per sec per cm^3 for 1 MW/m^2 wall loading; After 2 year operation)

		TIME AFTER SHUTDOWN						
Nuclide	Half-Life	0	10 m	1.7 h	2 yrs	20 yrs	200 yrs	2000 yrs
^{55}Fe	2.6 y	.103+12	.103+12	.103+12	.618+11	.645+9		
^{51}Cr	27.8 d	.647+11	.647+11	.646+11				
^{54}Mn	303 d	.957+10	.957+10	.957+10	.193+10			
^{57}Co	270 d	.476+11	.476+11	.476+11	.802+10			
^{60}Co	5.26 y	.116+11	.116+11	.116+11	.901+10	.937+9		
^{58}Co	71.3 d	.161+12	.161+12	.161+12				
$^{60\text{m}}\text{Co}$	10.5 m	.296+11	.153+11					
^{57}Ni	36 h	.978+10	.975+10	.948+10				
^{56}Mn	2.58 h	.542+11	.519+11	.346+11				
^{52}V	3.7 m	.203+11						
^{63}Ni	92 y					.725+8	.199+8	
^{59}Ni	8×10^4 y							.818+5
^{53}Mn	2×10^6 y							.186+4
TOTAL [DPS/cm ³]		.515+12	.480+12	.443+12	.813+11	.166+10	.200+8	837+5

TABLE 2D

Specific Radioactivity in First Wall (Zone 3) of LLL Design

(In disintegrations per sec per cm³ for 1 MW/m² wall loading; After 2 year operation)

		TIME AFTER SHUTDOWN						
Nuclide	Half-Life	0	10	1.7 h	2 yrs	20 yrs	200 yrs	2000 yrs
⁵⁵ Fe	2.6 y	.819+12	.819+12	.819+12	.493+12	.514+10		
⁵¹ Cr	27.8 d	.374+11	.374+11	.374+11				
⁵⁴ Mn	303 d	.101+12	.101+12	.101+12	.203+11			
⁵⁷ Co	270 d	.111+12	.111+12	.111+12	.187+11			
⁶⁰ Co	5.26 y	.279+11	.279+11	.279+11	.217+11	.226+10		
^{60m} Co	10.5 m	.713+11	.369+11					
⁵⁸ Co	71.3 d	.409+12	.409+12	.409+12				
⁵⁷ Ni	36 h	.233+11	.232+11	.226+11				
⁵⁶ Mn	2.58 h	.540+12	.516+12	.344+12			.452+8	
⁶³ Ni	92 y					.164+9		
⁵⁹ Ni	8x10 ⁴ y							.208+6
⁵³ Mn	2x10 ⁶ y							.214+5
TOTAL [DPS/cm ³]		.215+13	.209+13	.187+13	.554+12	.757+10	.454+8	.229+6

TABLE 2E
Specific Radioactivity In First Wall (Zone 3) of BNL Design
(In disintegrations per sec per cm^3 for 1 MW/m^2 wall loading; After 2 year operation)

TIME AFTER SHUTDOWN								
Nuclide	Half-life	0	10 m	1.7 h	2 years	20 yrs	200 yrs	2000 yrs
^{24}Na	15 h	.613+12	.608+12	.567+12				
^{27}Mg	9.5 m	.451+12	.217+12					
^{28}Al	2.3 m	.712+11						
$^{26\text{m}}\text{Al}$	6.4 s	.994+11						
^{16}N	7.1 s	.169+11						
^{26}Al	7×10^5 y				.184+6	.184+6	.184+6	.184+6
TOTAL [DPS/cm ³]		.125+13	.828+12	.568+12	.184+6	.184+6	.184+6	.184+6

Table 3
Effect of Branching Ratio Assumption on
Radioactivity and Afterheat in Nb

Time After Shutdown	Radioactivity (Ci/W _t)		Afterheat (Percentage of thermal Operating Power)	
	Case 1	Case 2	Case 1	Case 2
0	1.365	1.10	.217	.211
10m	.85	.76	.21-1	.186-1
1.7h	.71	.65	.16-1	.16-1
1 Wk	.41	.41	.99-2	.98-2
10 Wk	.12-1	.12-1	.26-2	.26-2
2 y	.13-2	.13-2	.49-4	.49-4
200 y	.45-4	.45-4	.47-4	.47-4

Case 1: Captures in ⁹³Nb and ⁹⁴Nb are assumed to lead to the metastable state 90% of the time

Case 2: Captures in ⁹³Nb and ⁹⁴Nb are assumed to lead to the metastable state 50% of the time.

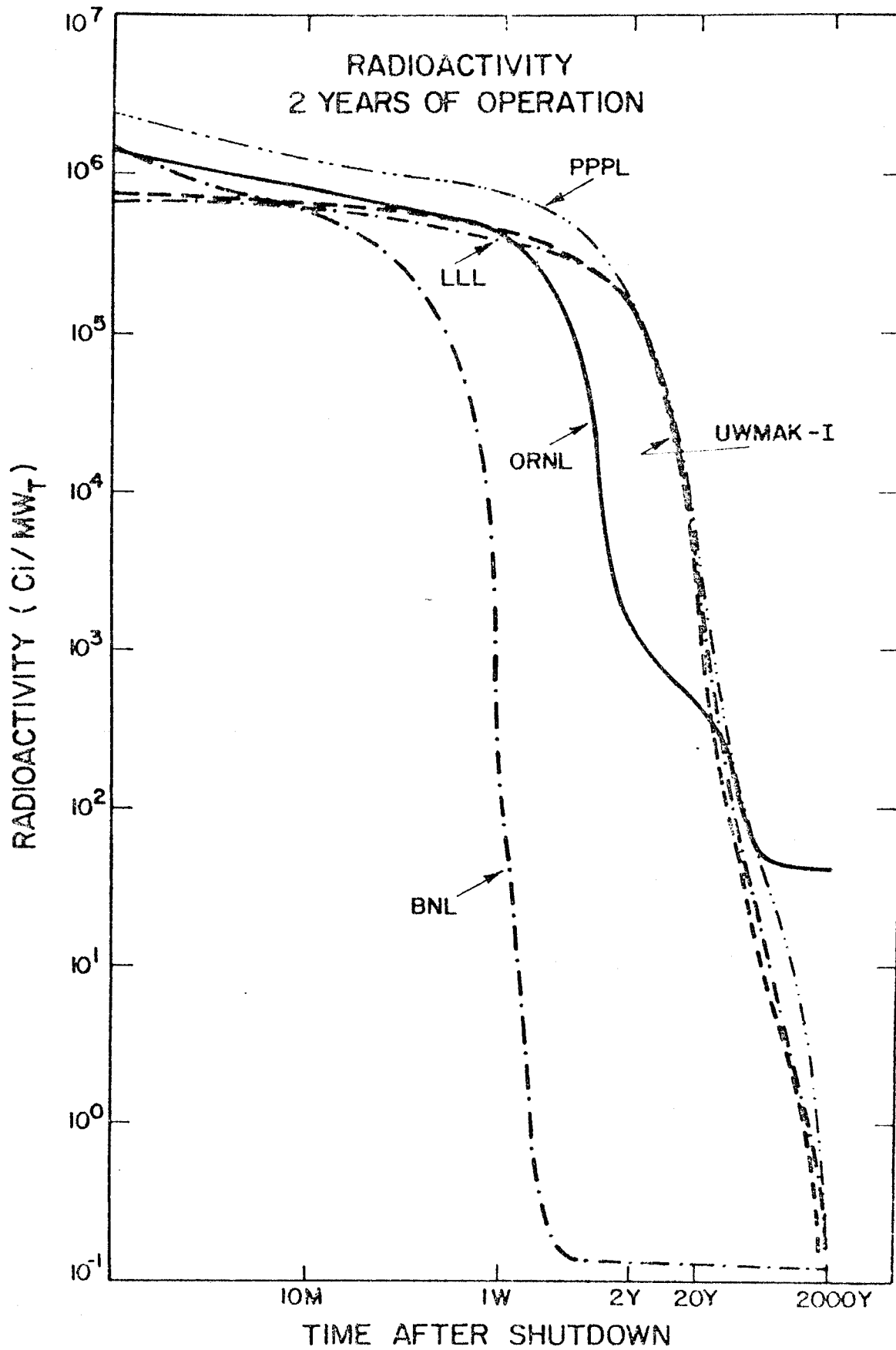


Fig.1

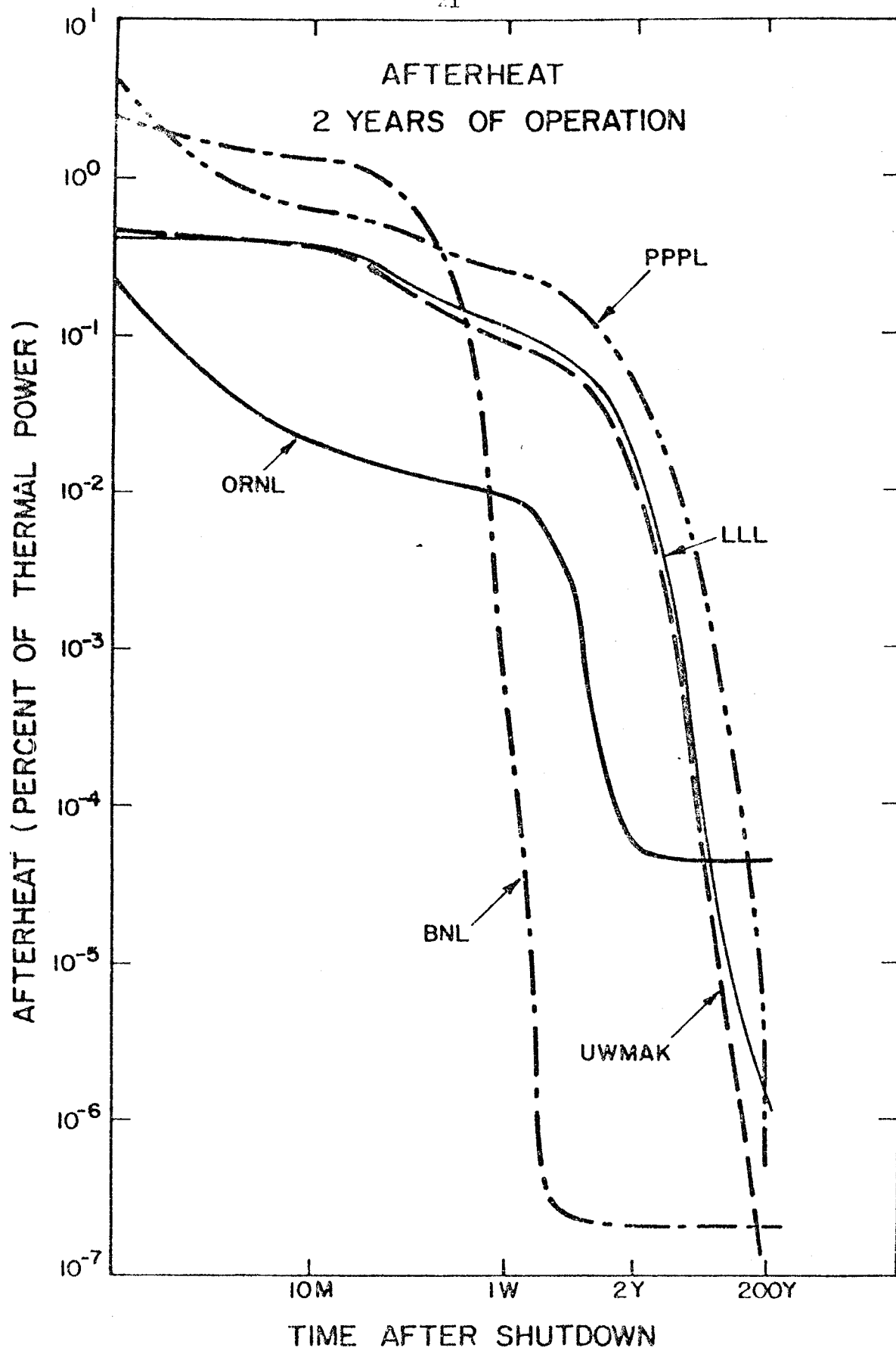


FIG. 2

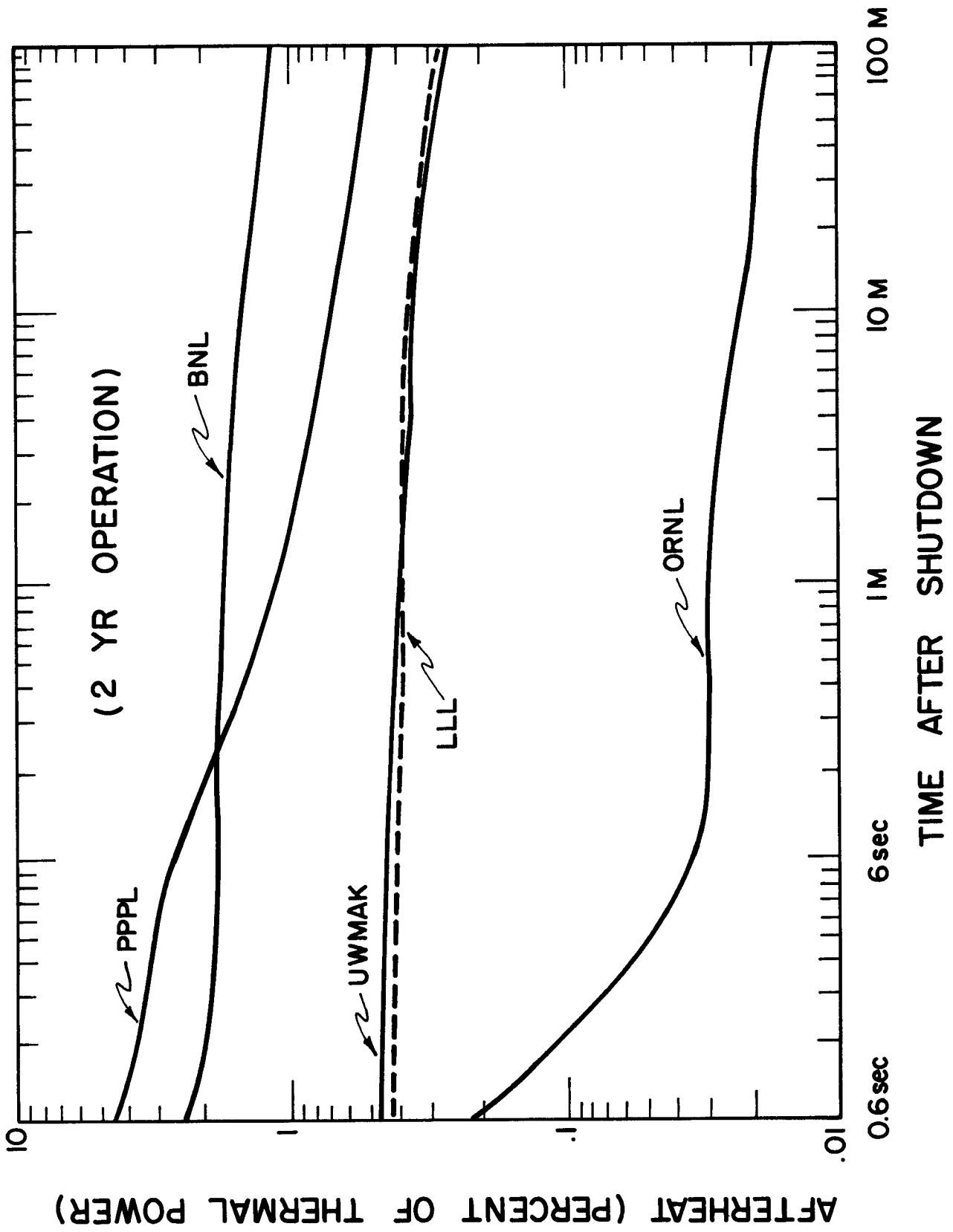


Figure 3

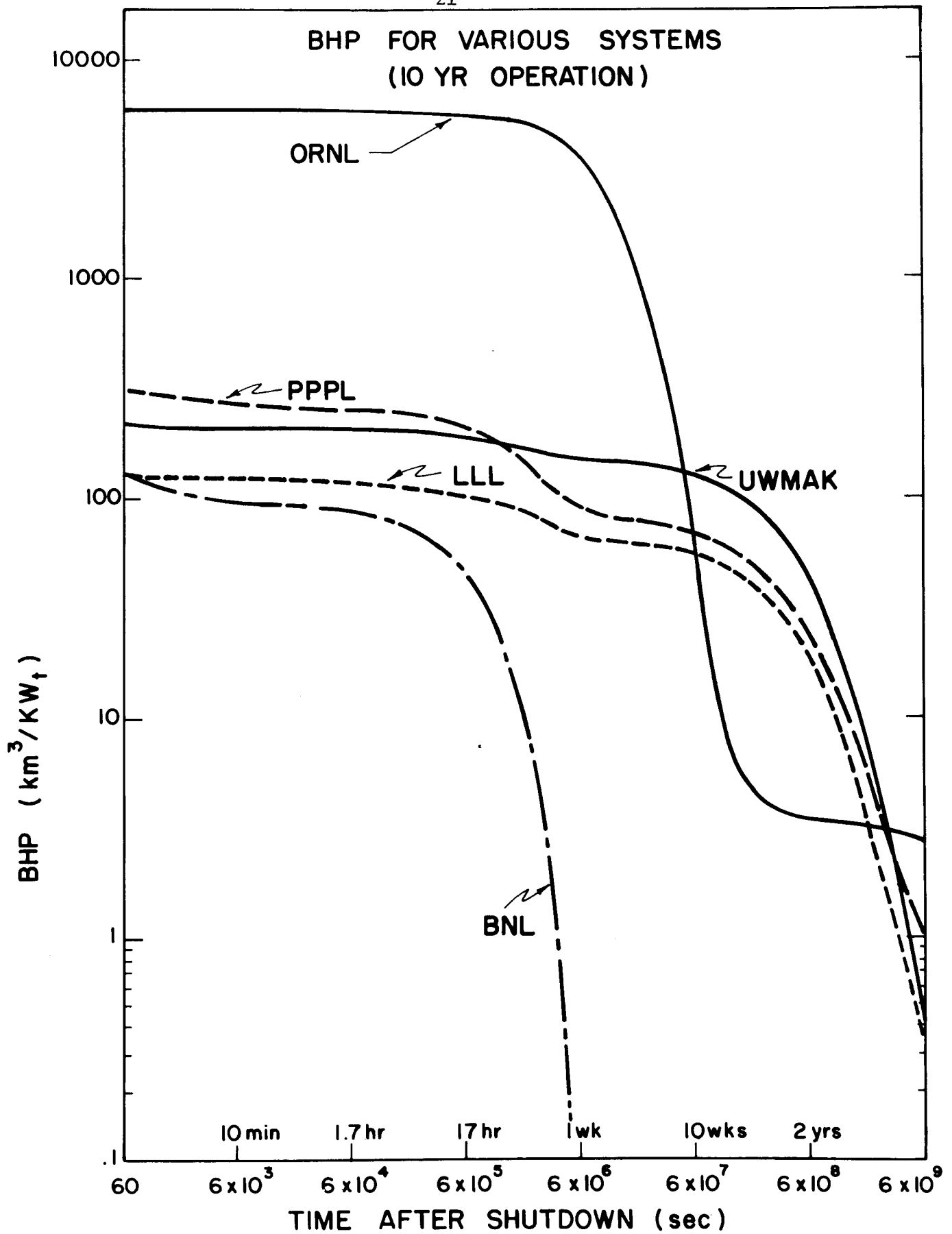


FIG. 4

FIG. 4

TIME AFTER SHUTDOWN (sec)